Full Articles

Study of the formation and stability of the Pd and Pt metallic nanoparticles on carbon support

A. Yu. Stakheev,[a]★ O. P. Tkachenko,[a] G. I. Kapustin,[a] N. S. Telegina,[a] G. N. Baeva,[a] T. R. Brueva,[a] K. V. Klementiev,[b,c] W. Grunert,[b] and L. M. Kustov[a]

[a]*Institute of Organic Chemistry, Russian Academy of Sciences, 47 Leninsky prosp., 119991 Moscow, Russian Federation. Fax: +7 (095) 135 5328. E-mail: st@ioc.ac.ru*
[b]*Ruhr-University Bochum, D-44780 Bochum, Germany*
[c]*Hasylab at DESY, D-22607 Hamburg, Germany*

Catalysts containing Pd and Pt on a Sibunit carbon support were studied by the temperature-programmed reduction, *in situ* X-ray photoelectron spectroscopy, and X-ray absorption spectroscopy (XAFS). The reduction of Pd and Pt species in samples 2%Pd/C and 2%Pt/C calcined in an air flow at 370 °C was studied. Reduction of the 2%Pd/C sample begins at 50—60 °C and is completed at 250—300 °C. Particles of various dispersion are formed during reduction. Long-distance peaks observed in the EXAFS spectra point to the presence of a fraction of relatively large crystallites. The average Pd—Pd coordination number (~5) at 200 °C gives evidence that a number of very small Pd nanoparticles, oligomeric clusters, is present. Reduction at $T > 200$°C results in sintering of a small fraction of the Pd particles. Reduction of Pt in 2%Pt/C sample begins at 120—150 °C and is completed at 300—350 °C. The sintering-resistant monodispersed Pt particles are formed under these conditions.

Key words: temperature-programmed reduction, X-ray photoelectron spectroscopy, X-ray absorption spectroscopy, reduction, catalysts Pd/C, Pt/C.

Carbon-based systems are very stable to aggressive media. On manufacturing catalysts for many chemical processes[1] carbon supports are therefore superior to conventional supports such as Al_2O_3 and SiO_2. Applying various treatments of carbon supports, one can control their porosity to obtain systems with a developed surface.[2—4] This allows the chemically inert carbon systems to be used as supports for transition metals.[5,6] In particular, the Pt/C and Pd/C catalysts are widely used in reactions involving dihydrogen, such as hydrogenation, dehydrogenation, and hydrogenolysis.

Highly-dispersed carbon-supported noble metals are of interest not only because of their function as conventional catalysts but also as the main components of hydrogen fuel cells. Pure platinum or that alloyed with other metals (Ru, Cr, Fe, Mn, Co, *etc*) and supported by a

Published in Russian in *Izvestiya Akademii Nauk. Seriya Khimicheskaya,* No. 3, pp. 502—511, March, 2004.
1066-5285/04/5303-0528

carbon is an electrode for low-temperature hydrogen fuel cells.[7—10]

High dispersion of a noble metal is needed both in catalysis and electrochemistry to ensure high reaction rates at low metal loadings. The most efficient procedure of the synthesis of catalysts on carbon supports is the molecular dispersion of a precursor of the metallic phase followed by reduction under controlled conditions. Anchoring the metal precursors is known to depend on both the nature of the surface oxygen-containing species of the carbon support and the deposition procedure.[6,11—13]

Two methods are known for anchoring platinum and palladium on supports. In the most abundant method[14] of deposition of Pd and Pt on carbon supports, H_2PdCl_4 and H_2PtCl_6 acids are used as the metal precursors.

We have developed an alternative procedure[15] that involves deposition of platinum and palladium as cations; the procedure allows molecular dispersion of cations on the surface of conducting graphitized carbon of the Sibunit type. The method based on preliminary mild oxidation of the Sibunit surface followed by the ion exchange of the transition metal cations allows one to achieve the molecular dispersion of cations on the support surface and stabilization of highly dispersed metallic particles during cation reduction.

This work was aimed at the development of the procedure for the preparation of metallic particles (Pt and Pd) with small sizes on the surface of a conducting carbon material. In addition, it was of interest to study the reduction process and stability (resistance to sintering) of the supported Pd and Pt clusters by temperature-programmed reduction (TPR), X-ray photoelectron spectroscopy (XPS), and X-ray absorption spectroscopy (XAFS).

Experimental

Catalyst synthesis. To prepare the 2%Pd/C and 2%Pt/C catalysts, we used a 0.3—1 mm fraction of the graphitized carbon support Sibunit prepared in Boreskov Institute of Catalysis, Siberian Branch of the Russian Academy of Sciences. Before the metal deposition, Sibunit was oxidized with a 0.2 *M* $KMnO_4$ solution followed by treatment with 4 *M* HCl.[15] Palladium and platinum were introduced by ion exchange in aqueous solutions of the $[Pt(NH_3)_4]Cl_2$ and $[Pd(NH_3)_4](NO_3)_2$ complexes at 20 °C for 3 h under continuous stirring. Then the catalysts were washed, dried at 120 °C, and calcined in an air flow at 370 °C (air flow rate 300 mL min^{-1}) for 2 h (rate of temperature raise 0.2 deg min^{-1}).

Characterization of the support texture. The textural characteristics of Sibunit were calculated from the adsorption isotherms of benzene vapor measured on a gravimetric adsorption setup at 20 °C. To calculate the specific surface area by the Brunauer—Emmett—Teller (BET) method, we accepted the benzene molecular area equal to 0.41 nm^2. The density of liquid benzene under specified conditions was taken for the calculation of the pore volume. The pore radius distribution curves were calculated according to the Kelvin equation for the model of cylindrical pores with the correction for the thickness of the adsorption film.[16] The textural characteristics were analyzed by constructing comparison plots[17] to determine micropores in the sample and calculate their specific surface area. A large-pore aluminosilicate with the specific surface area of 105 $m^2\ g^{-1}$ was used as the reference sample. The presence of supermicropores and micropores was revealed from the difference between the total pore volume and that of mesopores determined by integrating the pore radius distribution curves.

Temperature-programmed reduction. In these runs, a ~100 mg sample was treated with Ar at 300 °C for 1 h, cooled to ~20 °C, and then heated to 800 °C with a rate of 10 deg min^{-1} in an H_2—Ar gas flow (30 mL min^{-1}) containing 4.6 vol.% H_2. To remove water from the gas phase formed upon reduction, a trap cooled to 100 °C with a liquid nitrogen—ethanol mixture was placed between a reactor and a detector. The thermal-conductivity detector was calibrated by the reduction of CuO (Aldrich-Chemie GmbH, 99.99%) previously treated in an Ar flow at 300 °C. The deconvolution of the TPR peaks to components was carried out with the use of the program Origin, Peak Fitting module, Microcal Software Inc.

X-ray photoelectron spectra (Pd3d, Pt4f, and C 1s) were recorded on an XSAM-800 spectrometer with a Mg-$K\alpha_{1,2}$ radiation. The C 1s line with a binding energy of 285.0 eV was used as standard. The catalyst samples were reduced *in situ* in an H_2 flow in the temperature range 20—300 °C for 15 min and were placed into the chamber of the spectrometer avoiding contact with air. This *in situ* reduction procedure, spectra recording, and their processing and calculation have been described earlier.[18]

X-ray absorption spectra (XAFS). The XAFS spectra consist of two main parts. The first part is a spectrum region near the absorption edge (XANES). The second part of the XAFS spectra is defined as extended fine structure of X-ray absorption (EXAFS) and includes energies above 50 eV relative to the absorption edge. The XAFS spectra were recorded on an EXAFS station of the X1 laboratory HASYLAB in the DESY center of synchrotron radiation, Germany. The double crystal Si (311) monochromator was used. Before measurements, the energy scale of the monochromator was calibrated with an accuracy of 0.01 eV with the use of the tabular data for the PdK- and PtL_3-electron shells. The energy resolution was evaluated from ahgular beam size at 7.1 eV for PdK-edge (1s electrons) and at 1.6 eV for PtL_3-edge ($2p_{3/2}$ electrons). The transmission spectra were recorded at the temperature of liquid nitrogen in a He flow. In the XANES region, the spectra had a constant step of the photon energy (0.2 eV for Pd and 0.5 eV for Pt), whereas in the EXAFS region, the constant step of the wave vector of photoelectrons was the same for both edges and was equal to 0.025 $Å^{-1}$.

All the spectra were measured 2—3 times to check reproducibility and to collect the statistical data set. The samples were reduced *in situ* in a special chamber with a gas mixture containing 5 vol.% H_2 in He, which was fed in the EXAFS cell through a purification system. The samples of the 2%Pd/C catalyst were treated with pure He after each reduction at the same temperature in order to remove the palladium hydrides that formed upon hydrogen treatment. The catalyst samples represented pellets embedded into the pellet holder.

The EXAFS spectra were processed with a program VIPER for Windows.[19] To separate a change in the section of photoionization due to the atom under study from the change, which is due to back scattering from the neighboring atoms, we introduced the EXAFS function χ, which can be determined from

the absorption coefficient μ, and wieghted it by k^2 in the range of wavenumbers 2.75—16.45 Å^{-1} (Pd) and 4.00—16.85 Å^{-1} (Pt).

To obtain the quantitative data from the EXAFS spectra, we simulated the contributions from signals of the shells to the total signal, which were separated from the total signal by the Fourier transformation with the use of the known EXAFS formula in the harmonic approximation:

$$\chi = S_0^2 \sum_j \frac{N_j F_j(k)}{kR_j^2} \exp(-2\sigma_j^2 k^2) \sin[2kR_j + \phi_j(k)],$$

i.e. by summing up the atomic shells with the number j, where F are the scattering amplitudes and ϕ are the scattering phases from the neighboring atoms calculated *ab initio* with the FEFF8.10 code[20] and tested on the EXAFS spectra of the standards, Pd- and Pt-foils.

The experimental and theoretical spectra were compared in both vector k- and radial r-spaces. The fitting parameters for the experimental and theoretical spectra were interatomic distance (shell radius) R_j, coordination number N_j, the Debye—Waller factor σ^2_j, and adjustable "muffin-tin zero" ΔE_j. The multiple-excitation reduction factor was used as calculated by the FEFF8.10 code (S_0^2(Pd) = 0.923, S_0^2(Pt) = 0.934). Errors of the fitting parameters were found by the expansion of the statistical function χ^2 near its minimum, taking into account the maximal pair correlations.

The formal average radius of a metallic cluster (R/Å) was calculated from the EXAFS data according to the expression[21]

$$(CN)_{cluster} = (CN)_{crystal}(1 - 3/4\rho + 1/16\rho^3),$$

where $\rho = r/R$, r/Å is the interatomic distance in the first coordination sphere (Pd—Pd or Pt—Pt), $(CN)_{cluster}$ is the coordination number of the first coordination shell, and $(CN)_{crystal} = 12$ for the face-centered structures of platinum and palladium.

Results and Discussion

Study of reduction process

The textural characteristics of the initial and oxidized Sibunit samples are presented in Table 1. Only negligible decrease in the specific surface area is observed upon the oxidation of the parent Sibunit. The oxidative tratment of Sibunit causes a slight increase in the micropore volume, whereas the total pore volume decreases. No super-

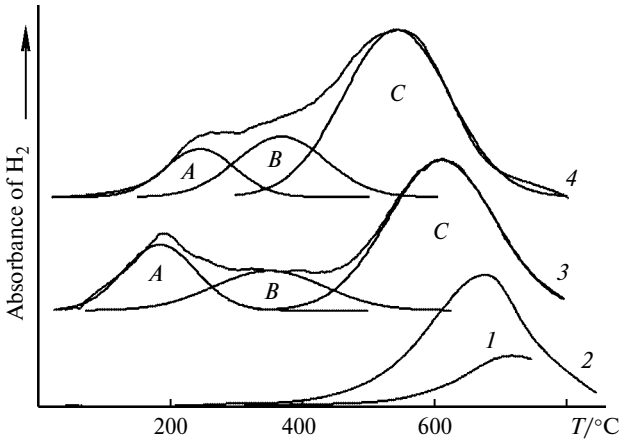

Fig. 1. Curves of temperature-programmed reduction of the initial (*1*) and oxidized (*2*) carbon supports, catalysts Pd/C (*3*) and Pt/C (*4*); *A*, *B*, and *C* are the Gaussian expansion peaks of the TPR curve.

micropores were found in both initial and oxidized Sibunit samples.

The profiles of the temperature-programmed reduction of the Pd/C and Pt/C catalysts previously calcined in air to remove ammonia ligands, as well as those of the initial and oxidized carbon support Sibunit are shown in Fig. 1. One broad peak with a maximum at 680 °C is seen on the TPR profile of the oxidized Sibunit (curve *2*). The appearance of this peak can be due to several reasons.

First, it is known[1] that the CO and CO_2 desorption from the surface of carbon supports due to the reduction of oxygen-containing groups is observed in this temperature region. The number of these groups increases with oxidation degree of the carbon support surface and the CO and CO_2 desorption increases consequently. This agrees with our earlier findings that the desorption peak has a considerably larger area than that for the initial unoxidized sample (curve *1*). Second, desorbed CO can cause a decrease in the thermal conductivity of the flow of H_2/Ar mixture, and this can be taken for the hydrogen uptake. In addition, when the oxygen-containing groups are removed, the unsaturated surface sites can be formed capable of adsorbing hydrogen.[1,22] Third, gasification of

Table 1. Textural characteristics of Sibunit

Sample	S_{BET}	S_{av}*	Pore volume**/cm^3 g^{-1}				
	m^2 g^{-1}		micropores with r < 7 Å	mesopores with various r/Å			total
				15—25	25—40	40—500	
Initial	466	424	0.015	0.205	0.142	0.355	0.717
Oxidized	399	349	0.018	0.175	0.086	0.327	0.606

* Determined by the comparative method. ** r is radius.

the carbon surface to form methane can occur over this temperature region.[23]

The TPR profiles of the 2%Pd/C and 2%Pt/C catalysts (curves *3* and *4*, respectively) can be described by the sum of three Gaussian curves (*A*, *B*, and *C*). Region *C* corresponds to the TPR curve of the oxidized Sibunit in both samples. However, the maximum of this peak in the spectra of both catalysts is shifted to lower-temperature region than that in the spectrum of the support, and this shift is more pronounced in the case of the 2%Pt/C catalyst. The area of this peak for both catalysts is somewhat larger compared to that of the parent support. The occurrence of this peak is likely due to the gasification of the carbon support surface. The hydrogen activation and spillover on metallic Pd and Pt should facilitate carbon methanation.

Region *A* corresponds to the reduction of Pd and Pt species. Reduction of Pd ions begins at 60 °C and maximizes at 195 °C (curve *3*). This process is essentially completed at 250—300 °C. It is known that palladium can occur on the catalyst surface in the forms of both PdO and isolated Pd^{2+} ions located near sites capable of partially compensating their charge, as, for example, in zeolites.[24] The PdO phase is reduced at low temperatures, 0—20 °C, while the isolated Pd^{2+} cations are reduced at the temperature near 200 °C. The isolated Pd^{2+} cations in our sample can be located on the carboxylic groups of the carbon support surface through ion-exchanging protons by cations. As no peak for palladium reduction was observed in the TPR spectrum at room temperature, we suggest that no PdO phase is present in the 2%Pd/C catalyst. The H/Pd = 1.9 was calculated from the reduction peak for Pd^{2+} cations having a maximum at 195 °C. This indicates that ions are dominant forms of Pd species in this sample.

The TPR profile of the 2%Pd/C catalyst did not contain the H_2 desorption peak at 50—60 °C related to the decomposition of palladium β-hydride. The ability of palladium to form hydrides is well known.[4,25,26] After complete palladium reduction to the metal, hydrogen adsorption decreases.[27—29] The fact that no peak of the hydrogen desorption to the gas phase due to hydride decomposition was found provides further evidence of the absence of PdO in the calcined nonreduced 2%Pd/C catalyst.[24]

It is known[30] that platinum species are reduced at higher temperatuires than Pd ions. A maximum of the peak of Pt reduction on the TPR profile for the 2%Pt/C catalyst is observed at 250 °C, and the process is completed at 360 °C (curve *4*). The H/Pt ratio calculated from the area of this peak is ~2.2. This indicates that Pt^{2+} cations predominate in the initial oxidized sample.

Region *B* in the TPR spectra of the Pd/C and Pt/C catalysts can be attributed to a decrease in the hydrogen concentration in the H_2/Ar mixture upon reduction of the oxygen-containing surface groups (carboxylic, phenolic, lactonic, *etc*.) located near the metal particles. The presence of the metal particles favors the activation and spillover of hydrogen. As can be seen from a comparison of curves *3* and *4* (see Fig. 1), this process occurs more intensely in the presence of Pt than in the presence of Pd. The peak area in region *B* is larger for the Pt/C catalyst than for the Pd/C catalyst, whereas the platinum sample contains nearly two times less metal atoms than the palladium sample. The fact that the peak area in region *C* is larger for Pt/C than for Pd/C is likely due to a more intense hydrogen spillover on the Pt catalyst.

The Pd3d and Pt4f XPS spectra for the 2%Pd/C and 2%Pt/C catalysts are shown in Figs. 2 and 3. The binding energy of Pd3$d_{5/2}$ electrons in the initial calcined sample is 337.8 eV. Such a binding energy points to the presence of Pd^{2+} cations as the only species in the sample. This is in agreement with the TPR data for the Pd/C catalyst.

According to the TPR data, palladium reduction with hydrogen begins at ~50 °C (see Fig. 1). A shoulder with a binding energy of ~336 eV appears in the XPS spectra of Pd3$d_{5/2}$ electrons (see Fig. 2). When the reduction tem-

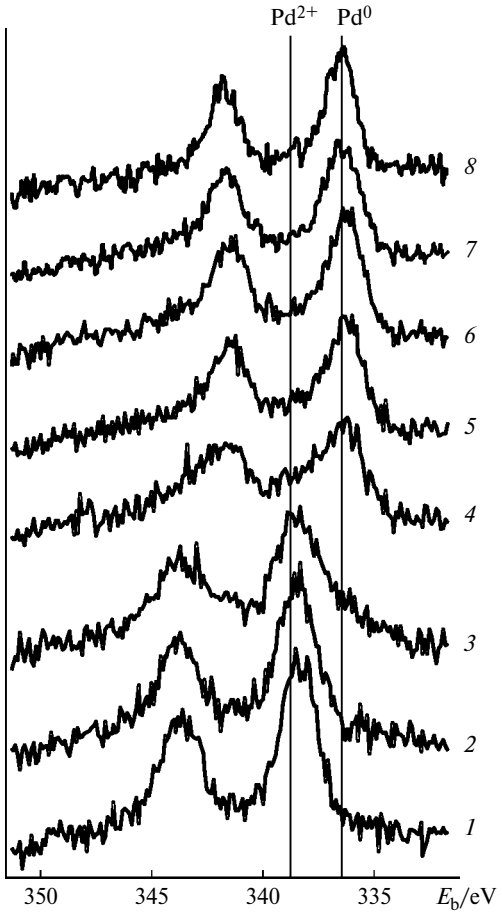

Fig. 2. The effect of temperature treatment in hydrogen on the binding energy (E_b) of Pd3d electrons in the 2% Pd/C catalyst: *1* is the initial sample, *2—8* are the samples heated to 20 (*2*), 50 (*3*), 100 (*4*), 150 (*5*), 200 (*6*), 250 (*7*), and 300 °C (*8*).

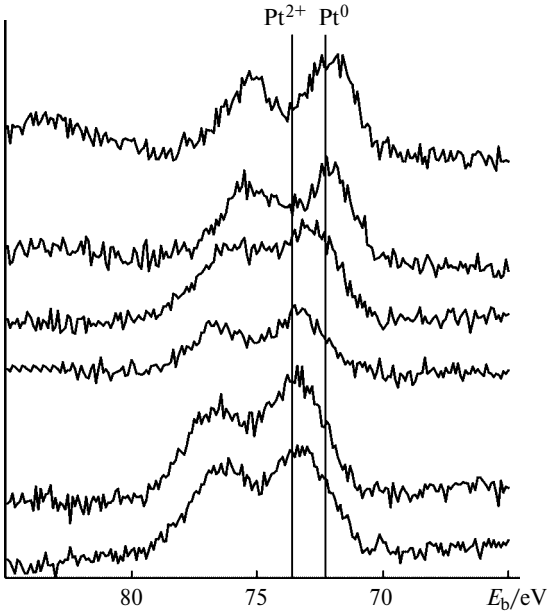

Fig. 3. The effect of reduction temperature or the binding energy of Pt4f electrons in the 2% Pt/C catalyst: *1* is the initial sample, *2—6* are the samples heated to 100 (*2*), 150 (*3*), 200 (*4*), 250 (*5*), and 300 (*6*).

perature is increased to 100 °C, a strong line with the binding energy (E_b) typical of metallic palladium is observed in the spectra of Pd3*d* electrons. However, the shape and width of this line again indicate the presence of nonreduced Pd^{2+} cations. Partial palladium reduction at this temperature is also seen at the TPR curves. With further increase in the temperature of hydrogen treatment from 150 to 300 °C, the lines of Pd3*d* electrons in the XPS spectra gradually become narrower and the only palladium state is observed at 250—300 °C that can be identified as Pd^0 with the binding energy of $Pd3d_{5/2}$ electrons equal to 336.3 eV. Palladium reduction is completed at 300 °C, and this agrees with the TPR data.

The binding energy of $Pt4f_{7/2}$ electrons in the XPS spectrum of the initial calcined Pt/C catalyst (see Fig. 3) is 73.5 eV. This value is typical of Pt^{2+} cations. Based on the XPS data, the reduction of platinum begins only at temperatures not lower than 150—200 °C, and this is confirmed by the TPR data. The two states of platinum, Pt^{2+} cations and Pt^0 are observed in the XPS spectra at 200 °C. It follows from the presence in the spectrum of Pt4f electrons of poorly resolved doublet with a maximum of the $Pt4f_{7/2}$ component at 73.0 eV. With further increase in the reduction temperature to 250—300 °C, the line of $Pt4f_{7/2}$ is shifted to lower binding energies down to 72.3±0.1 eV.

Hence, the TPR and XPS data showed that palladium is reduced completely in the temperature range of 50—200 °C and platinum is reduced at temperatures of 150—350 °C.

In addition, according to the XPS data, the binding energies of the core electrons of platinum and palladium in the initial calcined samples of the Pd/C and Pt/C catalysts are intermediate between those determined previously for the carrier-anchored ammino complexes of palladium and platinum $[Pd(NH_3)_4]^{2+}$ and $[Pt(NH_3)_4]^{2+}$, from one side, and supported oxides PdO and PtO in which both metals have the 2+ oxidation state, from the other side. The found E_b values of the $Pd3d_{5/2}$ and $Pt4f_{7/2}$ electrons in the initial calcined catalysts 2%Pd/C and 2%Pt/C are close to the corresponding values[18] for Pd^{2+} and Pt^{2+} grafted in the cavities of high-silica zeolites. The absence of the signal from nitrogen in the XPS spectra gives evidence of the complete decomposition and removal of palladium and platinum ammino complexes upon calcination.

Structure of metallic particles

The XAFS method was used to estimate the dispersion of the platinum and palladium crystallites and their resistance to sintering under high-temperature treatment with H_2. Before *in situ* experiments, the 2%Pd/C and 2%Pt/C catalysts were *ex situ* reduced with H_2 for 2 h at 200 °C and 350 °C, respectively.

The experimental XANES spectra for palladium *K*-edge absorption in the Pd/C catalyst and platinum L_3-edge absorption in the Pt/C catalyst recorded during high-temperature treatment with hydrogen are shown in Figs. 4 and 5. The radial distribution functions (without phase correction) obtained by the Fourier transform of the oscillating portion of the spectra for the Pd/C and Pt/C catalysts are presented in Figs. 6 and 7, respectively. The radial distribution functions for the Pd and Pt foils whose spectra were recorded under similar conditions are shown in the figures for comparison.

The structures of the nearest surrounding of palladium and platinum atoms in the catalysts calculated from the EXAFS data are presented in Table 2.

In the spectra of the supported catalysts (see Figs. 4, 5), no shifts of both Pd *K*-edge and Pt L_3-edge absorption relative to the edges corresponding to those for the bulk metals are observed. The intensities of white lines in the spectra of the Pd/C and Pt/C catalysts and in the spectra of Pt and Pd foils are comparable. Hence, the XANES spectra, in combination with the TPR and XPS data, give evidence that the platinum and palladium cations are fully reduced to metals at the temperatures 200 and 350 °C, respectively.

Calculation of the EXAFS data for the reduced Pd/C and Pt/C catalysts revealed only palladium and platinum atoms, respectively, in the nearest surroundings of the absorbing atoms (see Table 2).

High-temperature treatment of 2%Pd/C catalyst with hydrogen. The Fourier-transforms of the EXAFS spectra of the Pd/C catalyst reduced at temperatures of

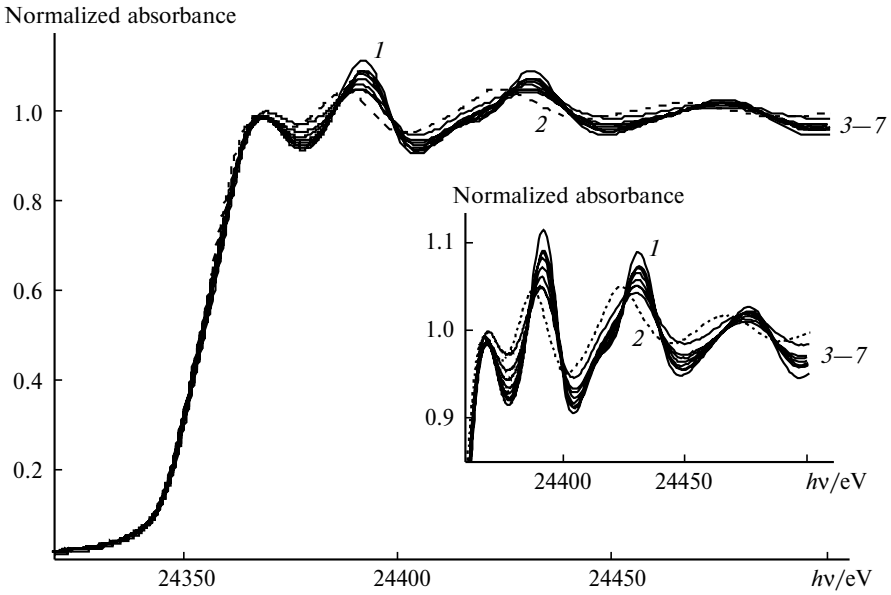

Fig. 4. Experimental XANES spectra of Pd foil (*1*), Pd hydride (*2*), and the Pd/C catalyst reduced at temperatures 200—500 °C (*3—7*).

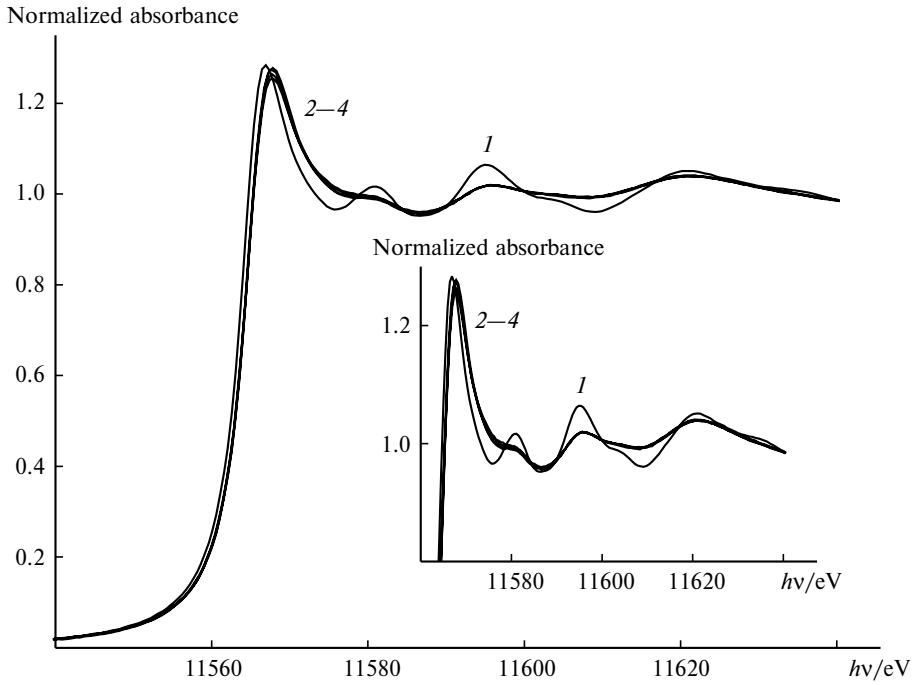

Fig. 5. Experimental XANES spectra of Pt foil (*1*) and the Pt/C catalyst reduced at temperatures 350—500 °C (*2—4*).

200—500 °C (see Fig. 6) contain a strong peak at r = 2—3 Å and several weaker long-distance peaks at r = 3—8 Å, which are similar to those in the spectra of Pd foil. The intensities of all the peaks gradually increase with increasing temperature of hydrogen treatment. Quantitative analysis of the EXAFS data for the Pd/C catalyst (see Table 2) shows that the metal particles are formed at the reduction temperature of 200 °C with the central Pd atom separated from the nearest neighboring five Pd atoms by the shortest interatomic distance (~2.73 Å) . The Pd—Pd coordination number gradually increases to 8.7 (Fig. 8, curve *1*) as the reduction temperature increases to 500 °C. At this reduction temperature, the neighboring palladium atoms occur at a distance of ~2.74 Å from the absorbing palladium atom.

Based on a spherical shape of particles, the formal size of palladium metal particles formed upon reduction on the Sibunit surface can be calculated. The size of the

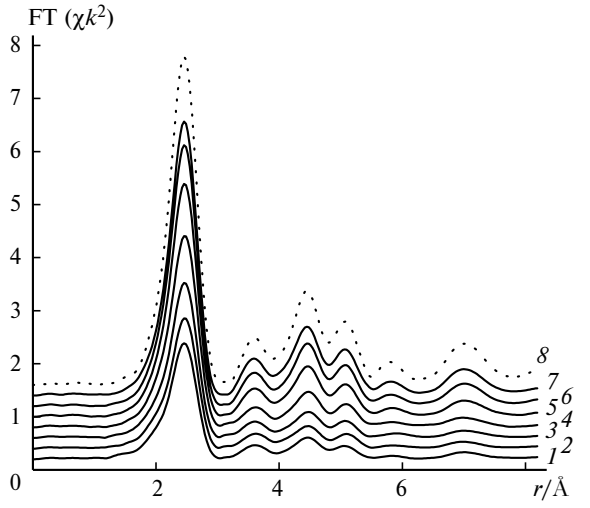

Fig. 6. Radial distribution functions calculated from the Fourier transform of the Pd*K*-edge of EXAFS spectra of the Pd/C catalyst reduced at various temperatures (*1*—*7*) and Pd foil (*8*): *1*, 200 °C, *2*, 250 °C, *3*, 300 °C, *4*, 350 °C, *5*, 400 °C, *6*, 450 °C, and *7*, 500 °C.

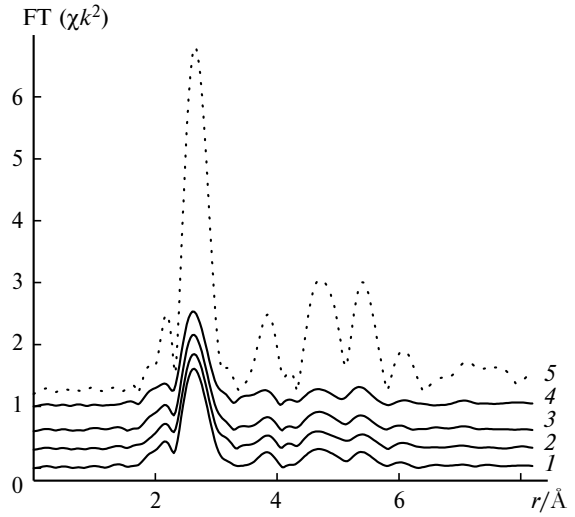

Fig. 7. Radial distribution functions calculated from the Fourier transform of the PtL_3-edge of EXAFS spectra of the Pd/C catalyst reduced at various temperatures (*1*—*4*) and Pt foil (*5*): *1*, 350 °C, *2*, 400 °C, *3*, 450 °C, and *4*, 500 °C.

metallic particles calculated from the EXAFS data can be correctly found only when the particles have nearly the same size and are small (<20 Å). Then the average formal size of palladium particles upon reduction at 200 °C will be ~7 Å and will increase to 15 Å with increase in reduction temperature to 500 °C.

From the formally calculated diameters of the palladium particles of 7—15 Å (see Table 2) one cannot conclude that only highly dispersed particles are present. The long-distance peaks on the radial distribution curve point to the presence of large particles on the surface of the Pd/C catalyst. These peaks are seen even in the spectra of the sample reduced at 200 °C. The intensities of all the peaks gradually increase and at 500 °C become comparable with those on the radial distribution curve for Pd foil.

The fact that the oscillation intensity in the spectra of the Pd/C catalyst (see Fig. 4) in the region close to the absorption edge are comparable to those in the XANES spectra of Pd foil in the same region, also confirm the presence of large metal particles on the catalyst surface.

Hence, the XAFS data on the reduction of the 2%Pd/C catalyst indicate that the palladium metal particles with various sizes are formed at temperatures as low as 200 °C. A fraction of the metal particles easily undergo sintering at higher reduction temperature. Larger particles are known to contribute most significantly to the average coordination number (CN) calculated from the EXAFS data. An increase in the formal average size of the palladium particles only to 15 Å gives evidence of the presence of a number of very small particles (metal oligomers) formed

Table 2. Data of the EXAFS spectra for the catalysts 2%Pd/C and 2%Pt/C reduced with H_2 at different temperatures

T/ °C	Catalyst	Atomic pair	*r*/Å	CN	σ^2 10^{-3}/Å^2	ΔE/eV	D_{Pt}, D_{Pd}*/Å
200	Pd/C	Pd—Pd	2.733±0.006	5.2±0.5	4.4±0.7	5±1	6.8±0.4
250	Pd/C	Pd—Pd	2.732±0.006	5.9±0.5	4.5±0.6	5±1	7.8±0.4
300	Pd/C	Pd—Pd	2.733±0.005	6.6±0.6	4.2±0.6	6±1	8.8±0.6
350	Pd/C	Pd—Pd	2.735±0.005	7.4±0.6	3.8±0.9	6±1	10.6±0.8
	Pt/C	Pt—Pt	2.745±0.003	7.6±0.4	5.5±0.4	9±1	11.0±2.1
400	Pd/C	Pd—Pd	2.738±0.004	8.0±0.6	3.2±0.5	6±1	12.2±0.8
	Pt/C	Pt—Pt	2.745±0.004	7.6±0.5	5.6±0.4	10±1	11.0±2.5
450	Pd/C	Pd—Pd	2.740±0.004	8.4±0.6	2.9±0.4	6±1	13.6±1.0
	Pt/C	Pt—Pt	2.749±0.003	7.5±0.4	5.5±0.3	10±1	10.8±1.9
500	Pd/C	Pd—Pd	2.742±0.008	8.7±0.6	2.8±0.7	6±1	15.0±1.0
	Pt/C	Pt—Pt	2.747±0.003	7.6±0.4	5.6±0.3	9±1	11.0±2.1
Pd foil	Pd/C	Pd—Pd	2.742±0.004	12.4±0.9	3.4±0.5	6±1	∞
	Pt/C	Pt—Pt	2.768±0.002	12.4±0.5	2.5±0.1	11±1	∞

* D_{Pt} or D_{Pd} is the calculated diameter of nanoparticles.

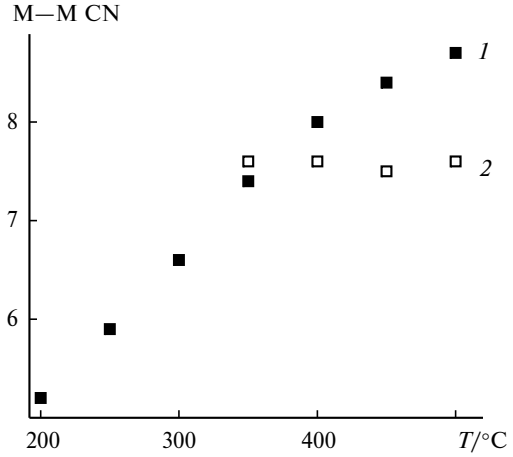

Fig. 8. Metal—metal CN in the catalysts supported on Sibunit *vs.* reduction temperature: *1*, Pd/C, *2*, Pt/C.

upon the hydrogen treatment of the 2%Pd/C catalyst even at 500 °C.

Calculation of the number of palladium atoms present in crystallites of different size from the Pd—Pd average CN, as it was done for platinum particles,[31] shows that the particles reduced at 200 °C contain in the mean 10—15 palladium atoms. At the reduction temperature 500 °C, the average number of palladium atoms in the particle increases to 100—150 (Fig. 9). It is obvious that under the conditions of low-temperature reduction, palladium mainly exists in the form of oligomers containing less than 10 palladium atoms. At the reduction temperature 500 °C, the number of large metal particles increases. The palladium dispersion defined as the ratio of the number of surface palladium atoms in the crystallite to the total number present decreases from 0.9 (200 °C) to 0.7 (500 °C).

Calculation of the EXAFS spectra clearly shows that the Pd—Pd interatomic distance in the reduced samples of the 2%Pd/C catalyst is less or coincides with that calculated from the standard spectrum of palladium foil recorded under similar conditions (2.74 Å) (see Table 2). It is well known[32] that the incorporation of hydrogen or carbon atoms into the metallic palladium lattice results in an increase in its parameters.[32] As the EXAFS data (Pd—Pd distance) and XANES data (position of K-edge of Pd absorption and the intensity of lines near it[28]) show, palladium hydrides and carbides are completely absent from the 2%Pd/C catalyst under the chosen reduction conditions. Palladium hydride is formed during reduction (see Fig. 4) but is removed by treatment with He. (More detailed description of the XAFS study of the formation and disintegration of palladium hydride will be reported in a separate article.)

High-temperature treatment of 2%Pt/C catalyst with hydrogen. Results of the treatment of the Pt/C catalyst prereduced at 350 °C with a hydrogen-containing mixture are presented in Figs. 5 and 7. A strong doublet in the region 2—3 Å that corresponds to the Pt—Pt distance and weak long-distance peaks in the region of 3—7 Å are observed on the Fourier-transform curve (see Fig. 7, curve *1*). Increasing the temperature of treatment with a hydrogen-containing gas mixture from 350 to 500 °C produces no changes on the radial distribution curves. As can be seen in Fig. 8 (curve *2*), the Pt—Pt coordination number is practically independent of the reduction temperature over this temperature range. Approximately eight platinum atoms comprise nearest surrounding of the ab-

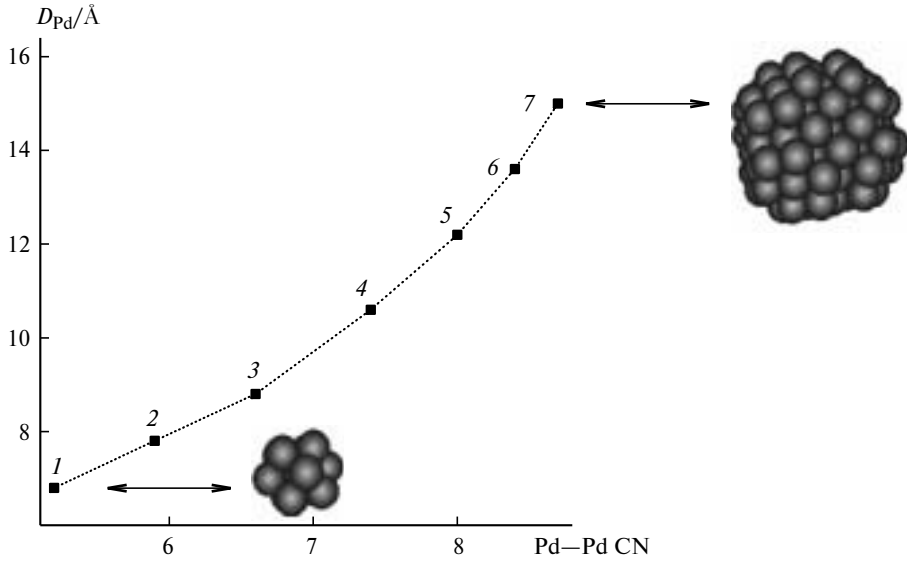

Fig. 9. Size of the Pd metallic nanoparticles in the 2%Pd/C catalyst reduced at different temperatures/°C: *1* — 200, *2* — 250, *3* — 300, *4* — 350, *5* — 400, *6* — 450, *7* — 500. Pictures of clusters were borrowed from work[31].

sorbing platinum atom (CN of Pt—Pt is 7.6) at a distance of ~2.75 Å (see Table 2).

The low intensity of oscillations in the region close to the edge of platinum absorption in the XANES spectra (see Fig. 5) indicate the presence of small metal particles. The intensity of these oscillations even upon treatment with hydrogen-containing mixture at 500 °C does not achieve the intensity of the same lines in the XANES spectrum of bulk platinum. The average size of platinum metal particles does not change, and its formal diameter remains ~11 Å (see Table 2).

Hence, the XAFS data obtained during the reduction of the 2%Pt/C catalyst indicate that the highly dispersed platinum metal particles are formed already at the reduction temperature as low as 350 °C. The platinum nanoparticles are very stable and do not undergo sintering with increase in the reduction temperature up to 500 °C.

The calculation of the number of platinum atoms that are present in the particles of a definite size from the average CN of Pt—Pt shows the particles containing in the mean ~50 platinum atoms are formed in the range of reduction temperatures of 350—500 °C.[31] The calculated dispersion of platinum metal nanoparticles remains approximately 0.9.

The calculation of the EXAFS spectra clearly shows that the Pt—Pt interatomic distance in the reduced samples of the 2%Pt/C catalysts (2.74—2.75 Å) is less than that calculated from the standard spectrum of Pt foil recorded under similar conditions (2.77 Å) (see Table 2). Hence, the Pt—Pt distance reveals that large particles with the structure of bulk platinum are completely absent from the 2%Pt/C catalyst upon the chosen reduction conditions.

The chosen procedure of the catalyst preparation by ion exchange of the platinum and palladium ammino complexes with the preoxidized Sibunit surface is suitable for the deposition of the isolated palladium and platinum cations on the surface of the carbon support without forming the corresponding oxide phases on the catalyst surface.

Palladium species in the 2%Pd/C catalyst begin reducing at 50—60 °C and are completely reduced to a zerovalent state at temperatures of 250—300 °C. The metallic palladium particles with various sizes are formed upon reduction. The long-distance peaks in the EXAFS spectra indicate the presence of the fraction containing relatively large particles. The average Pd—Pd coordination number (~5) at 200 °C gives evidence of the presence of a number of very small palladium nanoparticles (oligomeric clusters). The average dispersion of the Pd clusters decreases with further increase in the reduction temperature due to sintering of a small portion of the palladium particles. The average Pd—Pd coordination number in the particles reduced at 500 °C increases to 9 and the formal average diameter of the particles reaches a value of 15 Å.

In the 2%Pt/C catalyst, platinum species begin reducing at 120—150 °C and are fully reduced at temperatures of 300—350 °C. The monodispersed sinter-resistant Pt particles are formed under these conditions. The average Pt—Pt coordination number remains constant (~8) up to the reduction temperature of 500 °C. The formal average diameter of the platinum nanoparticles does not exceed 11 Å.

Based on the EXAFS data, it can not be inferred how high is the fraction of palladium atoms that form highly dispersed crystallites. Knowing the size of highly dispersed Pd particles, one can conclude that they are located in the support micropores whose diameter does not exceed 14 Å. As supermicropores (diameter 14—30 Å) were not found by the textural analysis in the Sibunit samples, one can suggest that larger palladium particles are located in the Sibunit mesopores (30—1000 Å). In their turn, practically all the platinum particles exist in the support micropores.

This work was performed in the framework of agreement between N. D. Zelinskii Institute of Organic Chemistry, Russian Academy of Sciences, and the Germany Center of Synchrotron Radiation (DESY, HASYLAB) (project I-02-013).

References

1. A. Sepulveda-Escribano, F. Coloma, and F. Rodriguez-Reinoso, *Appl. Catal. A*, 1998, **173**, 247.
2. M. Gurrath, T. Kuretzky, H. P. Boehm, L. B. Okhlopkova, A. S. Lisitsyn, and V. A. Likholobov, *Carbon*, 2000, **38**, 1241.
3. A. Dandekar, R. T. K. Baker, and M. A. Vannice, *Carbon* 1998, **36**, 1821.
4. N. Krishnankutty, J. Li, and V. A. Vannice, *Appl. Catal. A*, 1998, **173**, 137.
5. G. Neri, M. G. Musolino, C. Milone, A. M. Visco, and A. Di Mario, *J. Molec. Catal. A*, 1995, **95**, 235.
6. G. C. Torres, E. L. Jablonski, G. T. Baronetti, A. A. Castro, S. R. de Miguel, O. A. Scelza, M. D. Blanco, M. A. Pena-Jimenez, and J. L. G. Fierro, *Appl. Catal. A*, 1997, **161**, 213.
7. T. R. Ralph and M. P. Hogarth, *Platinum Metals Rev.*, 2002, **46**, 3.
8. D. S. Cameron, *Platinum Metals Rev.*, 2003, **47**, 28.
9. T. R. Ralph and M. P. Hogarth, *Platinum Metals Rev.*, 2002, **46**, 117.
10. M. P. Hogarth and T. R. Ralph, *Platinum Metals Rev.*, 2002, **46**, 146.
11. C. Prado-Burguete, A. Linares-Solano, F. Rodriguez-Reinoso, and de Lecea C. Salinas-Martinez, *J. Catal.* 1989, **115**, 98.
12. M. C. Roman-Martinez, D. Cazorla-Amoros, A. Linares-Solano, de L. C. Salinas-Martinez, H. Yamashita, and M. Ampo, *Carbon*, 1995, **33**, 3.
13. H. E. van Dam and H. van Bekkum, *J. Catal.* 1991, **131**, 335.
14. P. A. Symonov, A. V. Romanenko, I. P. Prosvirin, E. M. Moroz, A. I. Boronin, A. L. Chuvilin, and V. A. Likholobov, *Carbon*, 1997, **35**, 73.

15. A. Yu. Stakheev, G. N. Baeva, N. S. Telegina, A. B. Volynsky, L. M. Kustov, and Kh. M. Minachev, *Mendeleev Commun.*, 2000, 99.
16. M. M. Dubinin in *Metody issledovaniya struktury vysokodispersnykh i poristykh tel* [*Methods for the Study of the Structure of Highly Dispersed and Porous Materials*], Izd-vo Akad. Nauk SSSR, Moscow, 1958, 107.
17. A. P. Karnaukhov, *Adsorbtsiya. Tekstura dispersnykh i poristykh materialov* [*Adsorption. Texture of Dispersed and Porous Materials*], Nauka, Novosibirsk, 1999, 470 p.
18. Kh. M. Minachev and E. S. Shpiro, *Catalyst surface: Physical Methods of Studying*, Mir, Moscow, 1990, 375 p.
19. K. V. Klementiev, *VIPER for Windows (Visual Processing in EXAFS Researches)*, freeware, www.desy.de/~klmn/viper.html
20. A. L. Ankudinov, B. Ravel, J. J. Rehr, and S. D. Conradson, *Phys. Rev. B*, 1998, **58**, 7565.
21. M. Borowski, *J. Phys.*, 1997, IV 7, C2-259.
22. S. R. de Miguel, O. A. Scelza, M. C. Roman-Martinez, de Lecea C. Salinas-Martinez, D. Cazorla-Amoros, and A. Linares-Solano, *Appl. Catal. A*, 1998, **170**, 93.
23. A. Guerrero-Ruiza, P. Badenesb, and I. Rodrýguez-Ramosb, *Appl. Catal. A*, 1998, **173**, 313.
24. P. A. Weyrich, H. Trevino, W. F. Holderich, and W. M. H. Sachtler, *Appl. Catal. A*, 1997, **163**, 31.
25. S. B. Ziemecki and G. A. Jones, *J. Catal.*, 1985, **95**, 621.
26. S. B. Ziemecki, G. A. Jones, D. G. Swartfager, and R. L. Harlow, *J. Am. Chem. Soc.*, 1985, **107**, 4547.
27. S. Yu. Troitski, M. A. Serebriakova, M. A. Fedotov, S. V. Ignashin, A. L. Chuvilin, E. M. Moroz, B. N. Novgorodov, D. I. Kochubey, V. A. Likholobov, B. Blanc, and P. Gallezot, *J. Molec. Catal. A*, 2000, **158**, 461.
28. J. A. McCaulley, *J. Phys. Chem*. 1993, **97**, 10372.
29. N. Krishnankutty and M. A. Vannice, *J. Catal.* 1995, **155**, 312; 327.
30. J. R. Anderson, *Structure of Metallic Catalysts*, Academic Press, London, 1975.
31. J. de Graaf, A. J. van Dillen, K. P. de Jong, and D. C. Koningsberger, *J. Catal.*, 2001, **203**, 307.
32. R. K. Nandi, P. Georgopoulos, J. B. Cohen, J. B. Butt, and R. L. Burwell, *J. Catal.*, 1982, **77**, 421.

Received February 3, 2004;
in revised form March 3, 2004